

First demonstration of 200, 100, and 50 μm pitch Resistive AC-Coupled Silicon Detectors (RSD) with 100% fill-factor for 4D particle tracking

M. Mandurrino, R. Arcidiacono, M. Boscardin, N. Cartiglia, G. F. Dalla Betta, *Senior Member, IEEE*, M. Ferrero, F. Ficarella, L. Pancheri, *Member, IEEE*, G. Paternoster, F. Siviero, and M. Tornago

arXiv:1907.03314v1 [physics.ins-det] 7 Jul 2019

Abstract—We simulated, designed, produced, and tested RSD (Resistive AC-Coupled Silicon Detectors) devices, an evolution of the standard LGAD (Low-Gain Avalanche Diode) technology where a resistive *n*-type implant and a coupling dielectric layer have been implemented. The first feature works as a resistive sheet, freezing the multiplied charges, while the second one acts as a capacitive coupling for readout pads. We succeeded in the challenging goal of obtaining very fine pitch (50, 100, and 200 μm) while maintaining the signal waveforms suitable for high timing performances, as in the standard LGAD-based devices.

Index Terms—Silicon detectors, avalanche charge multiplication, timing, 4D tracking, LGAD, AC-coupled readout, RSD.

I. INTRODUCTION

RSD (Resistive AC-Coupled Silicon Detectors) are particle detectors with moderate internal gain based on the LGAD (Low-Gain Avalanche Diode) technology [1]. They are *n-in-p* sensors where an additional *p*-type layer, called multiplication or gain layer, is implanted under the *n*-type cathode. In reverse bias conditions, such layer provides an electric field which is responsible for the avalanche impact ionization of charge. Having an internal gain is beneficial, since the readout amplification would enhance also the electronic noise,

Submitted September 15, 2022; date of current version September 15, 2022. This work is supported by the Italian National Institute for Nuclear Physics, Gruppo V, through the framework of the RSD Project, by the Horizon 2020 Grants no. UFSID669529 and no. 654168 (AIDA-2020), by the U.S. Department of Energy, Grant no. DE-SC0010107, and by Dipartimenti di Eccellenza, University of Torino (ex L. 232/2016, art. 1, cc. 314, 337). Corresponding author: Marco Mandurrino.

M. Mandurrino and N. Cartiglia are with Istituto Nazionale di Fisica Nucleare, Sezione di Torino, Via P. Giuria 1, 10125 Torino, Italy (email: marco.mandurrino@to.infn.it).

R. Arcidiacono is with CERN, Esplanade des Particules 1, 1211, Meyrin, Switzerland, Universita' degli Studi del Piemonte Orientale, Largo Donegani 2/3, 28100 Novara, Italy, and Istituto Nazionale di Fisica Nucleare, Sezione di Torino, Via P. Giuria 1, 10125 Torino, Italy.

M. Boscardin, F. Ficarella, and G. Paternoster are with Fondazione Bruno Kessler, Via Sommarive 18, 38123 Trento, Italy, and TIFPA-INFN, Via Sommarive 18, 38123 Trento, Italy.

G. F. Dalla Betta and L. Pancheri are with TIFPA-INFN, Via Sommarive 18, 38123 Trento, Italy, and Universita' degli Studi di Trento, Via Sommarive 9, 38123 Trento, Italy.

M. Ferrero, F. Siviero, and M. Tornago are with Istituto Nazionale di Fisica Nucleare, Sezione di Torino, Via P. Giuria 1, 10125 Torino, Italy, and Universita' degli Studi di Torino, Via P. Giuria 1, 10125 Torino, Italy.

while the internal gain mainly provides signal multiplication, at least in the moderate gain regime. This increases the S/N (signal to noise) ratio and, even more interesting, allows to use the LGAD technology for timing applications. Indeed, higher gain increases the slew rate, which is strictly correlated to the time resolution [2]. Several simulations and measurements demonstrated that, for high-energy charged particles detection, a moderate gain ($G \sim 10\text{--}20$) in thin sensors ($\sim 50\text{ }\mu\text{m}$) allows to reach a time resolution of $\sim 30\text{ ps}$ [3], [4]. The other advantage of using the LGAD technology is the radiation tolerance: as it has been already proven on UFSID (Ultra-Fast Silicon Detectors, i.e. LGAD optimized for timing) this technology can operate in high-radiation environments, with fluence ϕ as large as $\phi \sim 10^{15}\text{ n}_{\text{eq}}/\text{cm}^2$ [5], which is fully compatible with the value expected in near-future hadron colliders (as the HL-LHC at CERN).

Since the onset of the LGAD multiplication process requires a large electric field ($\sim 300\text{ kV/cm}$), each pad has to be isolated with respect to the neighboring ones. To this purpose, the standard solution adopted is to implement segmentation structures between each pad which include all the implants needed to properly confine the electric field coming from each sensitive unit and to avoid short-circuits between them. Subfigure 1 (a) shows the inter-pad region between two LGAD structures, along with the JTE (junction termination extension) and *p*-stop segmentation implants. This strategy decreases the geometrical efficiency of the detector, because the segmentation structures introduce a discontinuity in the multiplication mechanism and, thus, a loss of efficiency in the track reconstruction.

To circumvent such problem we simulated, designed, produced and tested a run of RSD particle sensors [6], [7] within a collaboration among the Torino division of INFN (the Italian National Institute for Nuclear Physics), the University of Trento, and Fondazione Bruno Kessler (FBK). RSD are LGAD-based devices with unsegmented gain layer, which spreads throughout all the sensor area, which means a 100% fill-factor (the ratio between the active and the total area). The readout segmentation is obtained at the level of the AC metal pads, which are capacitively coupled to the detector bulk via a dielectric spacer layer deposited between the Silicon and the readout. The second working principle at the basis of RSD is the implementation of a *n*-type resistive implant beneath the

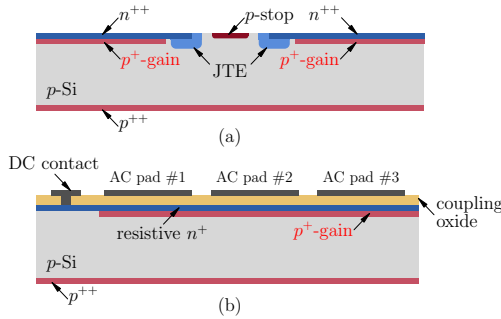


Fig. 1. Cross-section of an LGAD (a) in correspondence of the inter-pad region – where the JTE (junction termination extension) and the p -stop are the segmentation implants – and of an RSD (b).

coupling layer which allows (i) the induction of the signal in the AC metal pads and (ii) to control the slow discharge of the multiplied charges with a time constant given by the RC of the equivalent circuit. In particular, the discharge process is required to be sufficiently long to guarantee the complete signal induction, but also short enough to minimize pile-up effects [6].

II. DEVICES PRODUCTION AND TESTING

The spatial resolution in RSD is essentially determined by the pitch of the readout AC pads. For this reason we included in the first production run, named RSD1, various detector geometries, pitch and pad sizes, from more relaxed $500\text{ }\mu\text{m} \times 500\text{ }\mu\text{m}$ pitch square matrices to the finest ones with $50\text{ }\mu\text{m} \times 50\text{ }\mu\text{m}$ pitch. The goal is to find the best AC-related parameters, i.e. the dielectric thickness and the n -layer resistivity, which allow a proper reconstruction of the particle hit position in each of these designs.

TABLE I
SUMMARY OF PROCESS SPLIT PARAMETERS IN RSD1 BATCH

Wafer #	type	n^+ dose	p^+ dose	diel. thickness
1	FZ	A	0.92	L
2	FZ	A	0.94	L
3	Epi	A	0.94	L
4	FZ	A	0.94	H
5	FZ	A	0.96	L
6	Epi	B	0.92	L
7	FZ	B	0.94	L
8	FZ	B	0.94	L
9	FZ	B	0.96	L
10	FZ	B	0.96	H
11	FZ	C	0.92	L
12	Epi	C	0.94	L
13	FZ	C	0.94	L
14	Epi	C	0.96	H
15	FZ	C	0.96	H

To explore the phase-space of the RSD parameters, we processed 15 6" Silicon wafers with several splits of the most important implants (see Table I). In particular, the Boron dose in the gain layer spreads from 0.92 to 0.96, in steps of 0.02 each, where such numbers are in the same normalized scale of those reported in Table 1 of [5]. For what concerns the n -type cathode, we used a standard implantation dose (named B) which is approximately a tenth of that one used in all LGAD

presented in [5], plus two other splits, where this dose is halved (A) and doubled (C), respectively. Finally, the dielectric layer has been implemented only in two configurations, low (L) and high (H), by slightly changing the growth thickness during the deposition process.

After characterizing the production run at FBK through $I(V)$ and $C(V)$ measurements, which have shown a high homogeneity in terms of implantation doses, both within each wafer and among different wafers, the devices have been diced and then characterized in Torino with a IR laser ($\lambda \sim 1064\text{ nm}$) in a front-TCT (Transient Current Technique) equipment [8]. The laser illumination comes from the front side of the detector and, through ionization, generates a certain number of primary charges that undergo multiplication mechanism whose magnitude depends on the laser optical power, on the applied bias, and on the Boron dose in the gain layer.

All RSD devices have a DC collecting electrode surrounding the matrix of AC pads. Such DC-contact is grounded, while the reverse polarization is imposed by the voltage on the back side. The detector guardring (GR), collecting the leakage current coming from the device edges, is also connected to ground. Our testing campaigns involved several structures. Here we focus on the most challenging designs: the matrices with 3×3 pads of $200\text{ }\mu\text{m} \times 200\text{ }\mu\text{m}$, $100\text{ }\mu\text{m} \times 100\text{ }\mu\text{m}$, and $50\text{ }\mu\text{m} \times 50\text{ }\mu\text{m}$ pitch. The structures tested have $150\text{ }\mu\text{m} \times 150\text{ }\mu\text{m}$, $70\text{ }\mu\text{m} \times 70\text{ }\mu\text{m}$, and $35\text{ }\mu\text{m} \times 35\text{ }\mu\text{m}$ AC pad size, respectively. All the contacts have been realized through wire-wedge-bonding and the signals were read by broadband amplifiers (40 dB from CIVIDEC) concurrently from three AC pads while the others have been grounded, when possible.

III. RESULTS

The first device we present is the 3×3 pads matrix with $200\text{ }\mu\text{m} \times 200\text{ }\mu\text{m}$ pitch and $150\text{ }\mu\text{m} \times 150\text{ }\mu\text{m}$ pad size coming from wafer 10. After calibrating the laser focus, reaching a final spot with a diameter of about $15\text{ }\mu\text{m}$, the TCT laser scanned all the active part of the sensor, which has an area of $\sim 0.44\text{ mm}^2$. By integrating the AC signals coming from the three active channels for an integration time of about 5 ns, we obtained the 2D maps of charge reported in Figure 2.

As one may see, each channel shows a collection volume around its corresponding pad. This means that the overlap of neighboring collecting zones is such that it is possible to reconstruct the particle/laser hit position by weighting the number of charges induced on each channel of that cluster. Moreover, all the maps show the presence of the optical windows inside the AC pads, either square openings (as in the leftmost column) or slits with different orientations, that we designed in order to perform timing characterizations or specific inter-pad laser scans.

To study the 100 and $50\text{ }\mu\text{m}$ pitch RSD with the same laser setup, we measured samples from wafers 10 and 8, respectively. The resulting maps of charge, where the integration time is 3 ns for the $100\text{ }\mu\text{m}$ and 2.7 ns for the $50\text{ }\mu\text{m}$ pitch, are reported in Figures 3 and 4. In order to investigate the

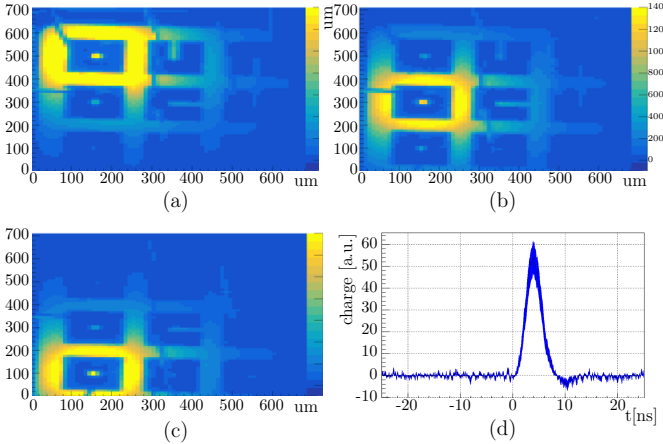


Fig. 2. 2D maps of induced charge obtained with a TCT setup after an integration time of about 5 ns for three different AC pads (a)–(c) of a 200 μm pitch RSD at 250 V (a typical value for a thin LGAD-based detector to operate); from the maps it is evident the presence of some optical windows (slits/spots) on the metal readout pads. Signal waveform produced by the same device (d).

segmentation properties of RSD1, for the 100 μm pitch sample we also took data with two floating AC pads and the signal did not degrade. For the 50 μm pitch detector, we also tested a sensor with three AC pads connected and six pads floating (without wire-bond). As in the previous case, no apparent differences have been observed with respect to the sensor with three pads connected and six pads grounded (through wire-bonding).

The effects of different RC on the signal shape can be seen comparing Figures 2(d) and 4(d): for higher RC the signal is larger with a smaller overshoot, consistent with our simulations [6], [7].

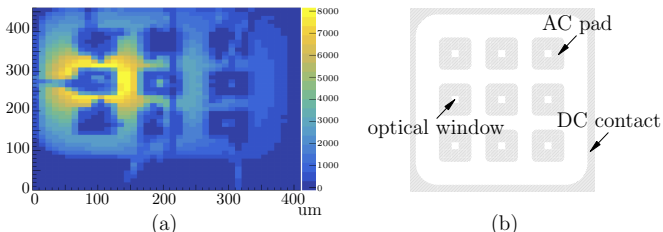


Fig. 3. 2D maps of induced charge in a 100 μm pitch RSD (a) obtained with a TCT setup at 250 V for a time integration of 3 ns and layout of the device (b).

Figures 2, 3, and 4 represent the first evidence, to the best of the author's knowledge, of a working ultra-fine-pitch segmentation in AC-coupled Silicon particle detectors with internal gain and 100% fill-factor.

REFERENCES

- [1] G. Pellegrini *et al.*, “Technology developments and first measurements of Low Gain Avalanche Detectors (LGAD) for high energy physics applications”, *Nucl. Instrum. Methods Phys. Res. A*, vol. 765, pp. 12–16, 2014, DOI: 10.1016/j.nima.2014.06.008.
- [2] N. Cartiglia *et al.*, “Beam test results of a 16 ps timing system based on ultra-fast silicon detectors”, *Nucl. Instrum. Methods Phys. Res. A*, vol. 850, pp. 83–88, 2017, DOI: 10.1016/j.nima.2017.01.021.
- [3] N. Cartiglia *et al.*, “Design optimization of UFSD silicon detectors”, *Nucl. Instrum. Methods Phys. Res. A*, vol. 796, pp. 141–148, 2015, DOI: 10.1016/j.nima.2015.04.025.
- [4] H. F.-W. Sadrozinski, A. Seiden, N. Cartiglia, “4D tracking with ultra-fast silicon detectors”, *Rep. Prog. Phys.*, vol. 81, p. 026101, 2018, DOI: 10.1088/1361-6633/aa94d3.
- [5] M. Ferrero *et al.*, “Radiation resistant LGAD design”, *Nucl. Instrum. Methods Phys. Res. A*, vol. 919, pp. 16–26, 2019, DOI: 10.1016/j.nima.2018.11.121.
- [6] M. Mandurrino *et al.*, “Resistive AC-Coupled Silicon Detectors (RSD). A new frontier in high-efficiency 4D particle tracking”, presented at the 2018 IEEE Nuclear Science Symposium and Medical Imaging Conference (NSS/MIC), Sydney, NSW, Australia, Nov. 10-17, 2018.
- [7] M. Mandurrino. (2019, June). First production of Resistive AC-Coupled Silicon Detectors (RSD) at FBK. Presented at the 34th RD50 Workshop. [Online]. Available: <https://indico.cern.ch/event/812761/contributions/3459062>
- [8] V. Eremin *et al.*, “Development of transient current and charge techniques for the measurement of effective net concentration of ionized charges (N_{eff}) in the space charge region of p-n junction detectors”, *Nucl. Instrum. Methods Phys. Res. A*, vol. 372, no. 3, pp. 388–398, 1993, DOI: 10.1016/0168-9002(95)01295-8.